Available online at www.sciencedirect.com

SciVerse ScienceDirect

Ceramics International 39 (2013) 925–930

CERAMICS INTERNATIONAL

www.elsevier.com/locate/ceramint

Effect of plastics substrate on phase separation behavior and adhesion for $RSi(OC_2H_5)_3$–$Si(OC_2H_5)_4$ coatings prepared by sol–gel process

Yutaka Mizuta, Yusuke Daiko, Atsushi Mineshige, Tetsuo Yazawa*

Department of Materials Science and Chemistry, University of Hyogo, Shosha, Himeji, Hyogo 671–2201, Japan

Received 11 May 2012; received in revised form 2 July 2012; accepted 2 July 2012
Available online 11 July 2012

Abstract

Three functional siliconalkoxides ($RSi(OC_2H_5)_3$, RTES), phenyltriethoxysilane (PhTES), methyltriethoxysilane (MeTES), and 1,4-bis(triethoxysilyl)benzene (BTEB)–tetraethoxysilane ($Si(OC_2H_5)_4$, TEOS) coatings [xA$-(100-x)$TEOS (x=0–80, mol%), A=PhTES, MeTES, BTEB] were prepared by sol–gel process, and the effects of plastics substrates on both the distribution of organic component in the coatings and its adhesion on plastics substrates were discussed. Polyethylene terephthalate (PET) and polycarbonate (PC) with phenyl group and polyethylene (PE), polypropylene (PP) and polyvinylchloride (PVC) without phenyl group were employed as plastics substrates. The distribution of organic component was monitored by total reflection (ATR) fourier transform infrared (FTIR) measurements. Before the solidification of the coating sol, the organic component for good adhesion migrated on coatings/substrate interface side by the interaction between organic component and substrate. This interaction may be caused by π/π electron interaction, CH_3/π electron interaction and CH_3/CH_3 van der Waals interaction. The migration of phenyl group on plastics substrate with phenyl group was larger than that on plastics substrate without phenyl group, while the migration of methyl group on plastics substrate without phenyl group was larger than that on plastics' substrates with phenyl group. Thus, the chemical structure of substrate affected phase separation behavior in the coatings. Adhesion of PhTES–TEOS and BTEB–TEOS coatings on PET and PC increased drastically at larger than x=60. On the other hand, no adhesion was observed for all the MeTES–TEOS coatings.

Keywords: A. Sol–gel processes; B. Nanocomposites; D. Silicate

1. Introduction

Polycarbonate (PC) has been widely used for its high transparency, good mechanical strength, high impact resistance and chemical stability. The application of PC as alternate glass-windows has also been considered [1]. One crucial aspect of PC for practical uses is its very low surface hardness of which pencil hardness is $\approx$4B.

Therefore, to improve the surface hardness, transparent hard coatings has been studied so far, including organic–inorganic hybrid coatings such as SiO_2, Al_2O_3, and TiO_2 [1–8]. In the hard coatings, not only hardness but also adhesion is very important. Even if the coatings with high surface hardness can be prepared, the coatings with poor adhesion easily peels off from plastics substrates.

We previously reported the adhesion and surface hardness of coatings on PC substrate prepared using phenyltriethoxysilane (PhTES) and tetraethoxysilane (TEOS) by sol–gel process [9–10]. As shown in Fig. 1, we anticipate the formation of phase separated structure in the coatings before its solidification of sol, namely organic component for good adhesion migrates on coatings/substrate interface side by the interaction between organic component and substrate, and consequently the inorganic one for hardness migrates on coating surface side by one-solution/one-step sol coating which is considered to be suitable to obtain functional coatings rapidly with low cost in practical uses.

In this paper, the relation between the distribution of organic component in the coatings and its adhesion on

*Corresponding author. Fax: +81 79 267 4896.
E-mail address: yazawa@eng.u-hyogo.ac.jp (T. Yazawa).

0272-8842/$36.00
http://dx.doi.org/10.1016/j.ceramint.2012.07.007

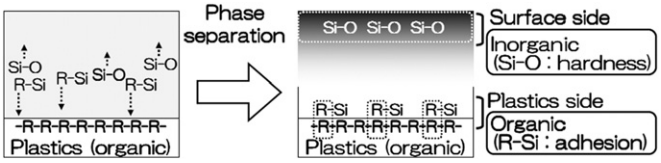

Fig. 1. Schematic illustration of phase separation behavior in coatings.

various plastics substrates with and without phenyl group are discussed.

2. Experimental

2.1. Preparation of sol solution

Hydrochloric acid of 0.1 wt% aqueous solution and ethanol were added to PhTES, (Aldrich Co.), methyltriethoxysilane (MeTES, Aldrich Co.) and 1,4-bis(triethoxysilyl)benzene (BTEB, Aldrich Co.) for hydrolysis, and the solution was stirred at 60 °C for 1 h. TEOS was added to the partially hydrolyzed PhTES, MeTES, and BTEB solution, and further stirred at 60 °C for 30 min. The chemical constitutionals of PhTES, MeTES, BTEB, and TEOS are shown in Fig. 2. The molar ratios of alkoxide:ethanol:H_2O:HCl were 1:5:4:0.002, and various compositions of coatings [xA−(100−x)TEOS (x=0–80, mol%), A=PhTES, MeTES, BTEB] were prepared. Plastics substrates with 2.5 cm × 1.5 cm × 1 mm thickness were used for the substrate. The chemical constitutionals of various plastics substrates employed are shown in Fig. 3. All coatings were prepared by dip-coating method with a withdrawing speed of 4.8 mm/s. After dried at room temperature for 10 min., the coated sample was dried at 60 °C for 2 h. Fig. 4 shows the photo of the typical example of PhTES–TEOS coatings on PC substrate.

2.2. Characterization of coatings

The distribution of organic components in the coatings was monitored by total reflection (ATR) fourier transform infrared spectroscopy (FT/IR-480 plus, JASCO Co.). ZnSe crystal (JASCO Co.) was used for the ATR measurement. The spectral domain for FT-IR measurement was 700–4000 cm^{-1}.

The thickness of the coatings was measured by surface profile measurement (Surftest SJ-401, Mitutoyo Co.) based on JIS B0601. The sensing pin was used for the standard stylus with 4 μm in diameter. The contact pressure of sensing pin for the thickness measurement was 0.75 mN.

The adhesion of coatings was measured by crosshatch adhesion test based on JIS K5600-5-6. The coatings were cut into 5 × 5 lines (25 boxes on the coating) by using a typical cross-cut guide (CCJ-2, COTEC Co.) with 2 mm spacing. A cellophane tape (CT-15, Nichiban Co.) covered on the coatings crosshatched. After 30–60 s, the cellophane tape was peeled off from the coatings. The adhesion (A) (%) was calculated as follows:

$$A = nad./25100 \quad (1)$$

where $n_{ad.}$ is the number of remaining boxes on coatings after the crosshatch test.

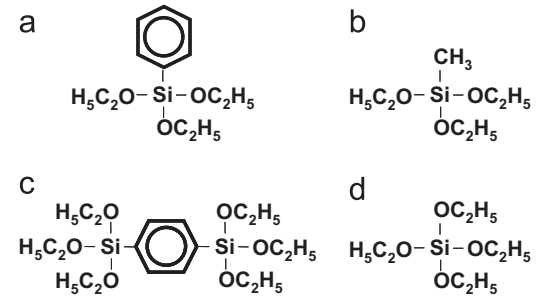

Fig. 2. Chemical constitutions of (a) phenyltriethoxysilane (PhTES), (b) methyltriethoxysilane (MeTES), (c) 1,4-bis(triethoxysilyl)benzene (BTEB), and (d) tetraethoxysilane (TEOS).

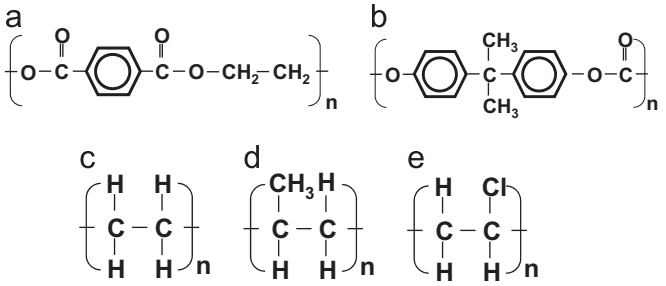

Fig. 3. Chemical constitutions of (a) polyethylene terephthalate (PET), (b) polycarbonate (PC), (c) polyethylene (PE), (d) polypropylene (PP), and (e) polyvinylchloride (PVC).

Fig. 4. Photo of typical example of PhTES–TEOS coatings on PC.

3. Result and discussion

3.1. Effect of substrate on distribution of organic component in coatings

The concentration of phenyl and methyl groups in the coatings on the surface side of substrates were estimated using ATR-FTIR technique as shown in Fig. 5. The thickness of all the coatings was summarized in Table 1.

It is clear that the thicknesses of all the coatings are approximately 2.0 μm. Since the IR penetration depth of our setup is approximately 1.3 μm, we can obtain only the surface side in coatings information. Consequently, the IR absorption of various plastics substrates was not observed.

Fig. 6 shows the typical ATR-FTIR spectra of PhTES–TEOS coatings with $x=20$ and 80. Two absorption bands due to the Si–O stretching of Si–O–Si network and C–Si stretching of phenyl groups were clearly observed at 1040 cm^{-1} and 1130 cm^{-1}, respectively [11–13]. In order to discuss the distribution of phenyl group, we defined a parameter α as follows:

$$\alpha = A_{C-Si}/(A_{C-Si}+A_{Si-O}) \quad (2)$$

where A_{C-Si} and A_{Si-O} are the absorbances at 1130 cm^{-1} and at 1040 cm^{-1}, respectively.

Changes in the α with composition x are plotted in Fig. 7. Throughout the x from 0 to 80, the α for coatings on polyethylene terephthalate (PET) and PC substrates with phenyl group was smaller than that for coatings on polyethylene (PE), polypropylene (PP) and polyvinylchloride (PVC) substrates without phenyl group at the same x. The decrease of α at the same x means that the amount of phenyl group on surface side of coatings decreased. Therefore, the migration of phenyl groups on plastics substrates side with phenyl group was larger than that on plastics substrate side without phenyl group.

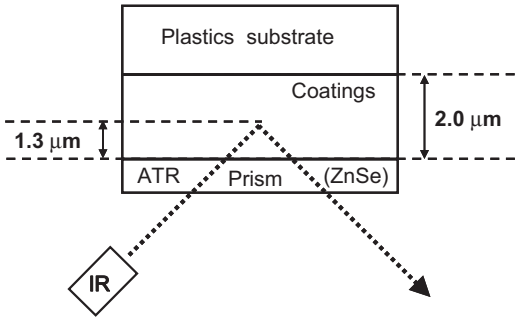

Fig. 5. Schematic illustration of ATR setup of FTIR measurement for coatings.

Fig. 8 shows the typical ATR-FTIR spectra of MeTES–TEOS coatings with $x=20$ and 80. Two absorption bands due to the Si–O stretching of Si–O–Si network and C–Si stretching of methyl group were clearly observed at 1040 cm^{-1} and 770 cm^{-1}, respectively [12]. In order to discuss the distribution of methyl group, we defined a parameter β as follows:

$$\beta = A_{C-Si}/(A_{C-Si}+A_{Si-O}) \quad (3)$$

where A_{C-Si} and A_{Si-O} are the absorbances at 770 cm^{-1} and at 1040 cm^{-1}, respectively.

Changes in the β with composition x are plotted in Fig. 9. Throughout the x from 0 to 80, the β for coatings on PE, PP and PVC substrates without phenyl group was smaller than that for coatings on PET and PC substrates

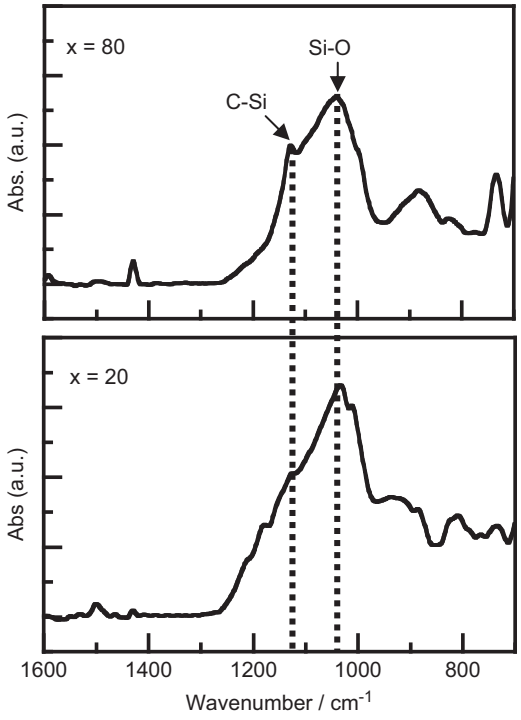

Fig. 6. ATR-FTIR spectra for PhTES–TEOS coatings with $x=20$ and 80 [x PhTES$-(100-x)$ TEOS (mol%)] dried at 60 °C.

Table 1
Thickness of all the coatings obtained.

RTES/ mol%	Thickness/μm									
x RTES$-(100-x)$TEOS	R=Ph					R=Me				
	PET	PC	PE	PP	PVC	PET	PC	PE	PP	PVC
0	1.8	2.0	2.1	1.8	1.9	1.8	2.0	2.1	1.8	1.9
10	1.7	2.0	2.2	2.1	1.9	1.7	1.7	1.8	2.0	2.1
20	1.7	2.0	1.8	1.8	1.7	1.7	1.7	1.8	2.0	2.0
30	1.7	2.0	2.2	2.2	1.8	1.9	1.9	1.7	1.8	1.8
40	1.8	1.8	2.0	2.2	1.7	1.9	1.7	1.7	1.8	1.8
50	2.0	2.0	2.1	2.2	1.8	1.7	1.7	1.8	1.8	1.8
60	2.0	1.7	2.1	2.2	1.7	2.0	2.0	2.0	2.0	2.0
70	2.2	1.8	2.2	2.1	2.2	1.9	1.9	2.0	1.9	1.7
80	2.0	2.0	2.2	2.1	2.2	1.9	2.0	1.8	1.9	1.8

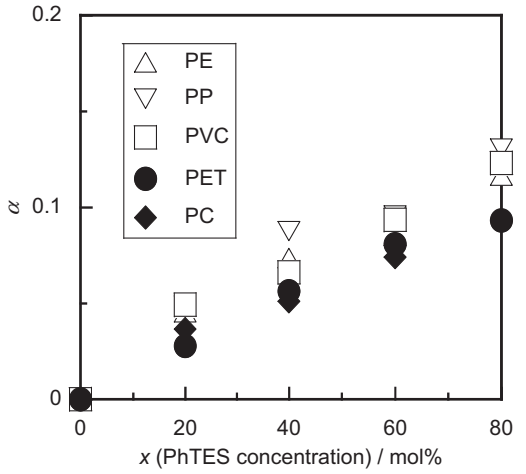

Fig. 7. Changes in α with composition x [x PhTES$-(100-x)$ TEOS (mol%)] coatings on various plastics substrates.

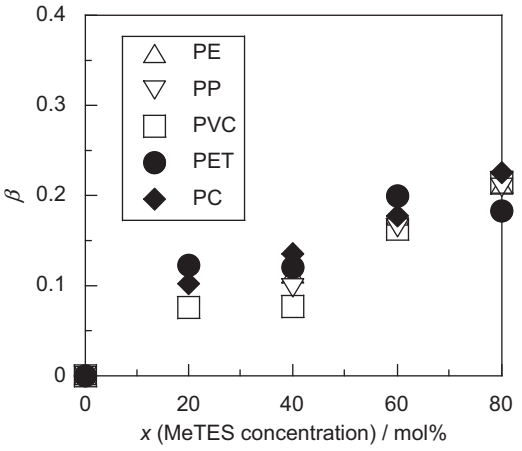

Fig. 9. Changes in β with composition x [x MeTES$-(100-x)$ TEOS (mol%)] coatings on various plastics substrates.

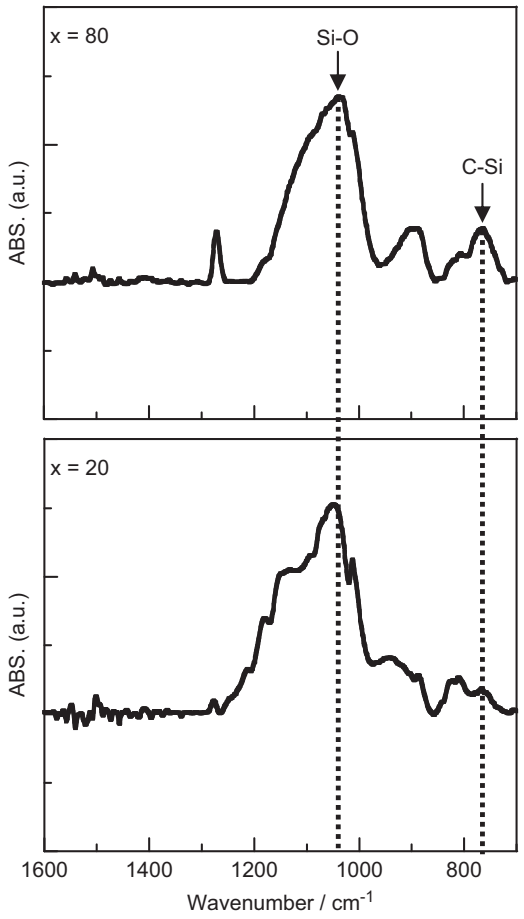

Fig. 8. ATR-FTIR spectra for MeTES-TEOS coatings with $x=20$ and 80 [x MeTES$-(100-x)$ TEOS (mol%)] dried at 60 °C.

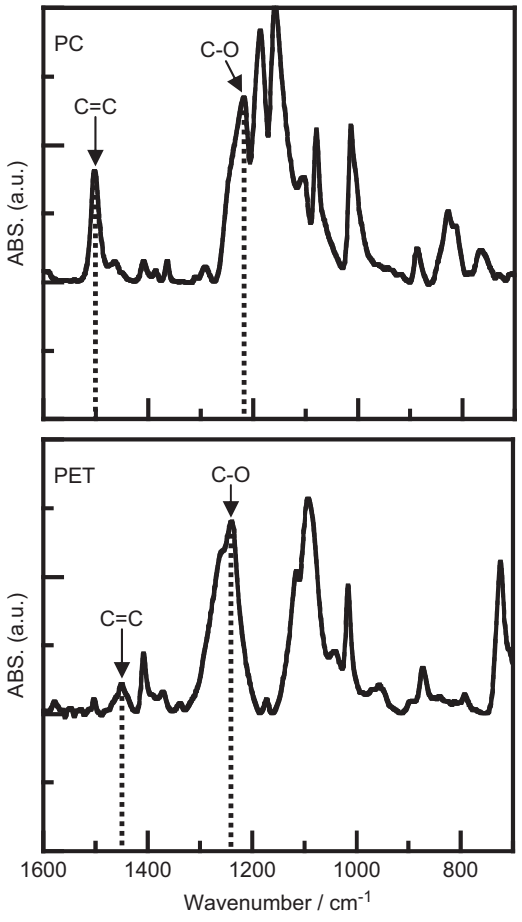

Fig. 10. ATR-FTIR spectra for PET and PC substrates.

with phenyl group. The decrease of β means that the proportion of methyl groups decreases on surface side. In both the cases of PhTES–TEOS and MeTES–TEOS, the α and β increased with increasing the x, whereas it is apparent that the slopes in Fig. 7 and Fig. 9 are not the same value. In the case of PhTES–TEOS sol, π/π electron interaction between the PhTES and substrate (PC or PET) is dominant, whereas the hydrophobic interaction between the methyl groups of MeTES and substrates (PE, PP, PVC) affects significantly on the migration of MeTES. The difference of the slopes in Fig. 7 and Fig. 9 may be considered to be related with the difference of these π/π electron or hydrophobic interaction.

As described above, it was clear that the chemical structure of substrate affected the distribution of organic component in the coatings. In other words, the chemical structure of substrate affected the phase separation behavior in the coatings. This may be caused by π/π electron interaction [14,15,17–19], CH_3/π electron interaction and CH_3/CH_3 van der Waals interaction [16–21] between the phenyl and methyl groups of the substrates and these groups in the coatings.

3.2. Effect of substrate on adhesion of coatings

Table 2 summarizes the compositions and results of adhesion test of PhTES–TEOS and MeTES–TEOS coatings on the various plastics substrates. Note that the adhesion of PhTES–TEOS coatings on PET and PC substrates with phenyl group increased drastically at larger than $x=60$. On the other hand, no adhesion (0%) was observed for all the MeTES–TEOS coatings. These results suggest no considerable interactions concerning adhesion between methyl group and all the substrates, PET, PC, PE, PP and PVC.

Further, as indicated in Table 2, for PhTES–TEOS coatings the adhesion was 40% on PET and 100% on PC at the same $x=60$. Since this difference may be attributed to the proportion of phenyl group in substrates, the adhesions of 4 kinds of PET with different proportion of phenyl group were investigated. The proportion of phenyl group in PET substrate was determined as follows: Fig. 10 shows the typical ATR-FTIR spectra for PET and PC substrate. Two absorption bands due to the C–O stretching of C–O–C and C=C stretching of phenyl groups were clearly observed at 1215 and 1500 cm^{-1} for PC and at 1240 and 1450 cm^{-1} for PET, respectively. Since C–O–C bond is in the same amount in its repeating molecular unit for PET and PC as shown in Fig. 3, the proportion of phenyl group in PET was determined based on the absorption ratio, $A_{C=C}/A_{C-O}$ for PC as indicated in the following equation:

$$Pphenyl = (AC=C/A_{C-O})PET/(A_{C=C}/A_{C-O})PC \times 100(\%) \quad (4)$$

As shown in Fig. 11, the adhesion of coatings was linearly increased by increasing the proportion of phenyl group of the substrates. Here, 60PhTES–40TEOS sol was employed for coating. Considering Table 2 and Fig. 11, good adhesion between organic component and plastics substrate may be caused by π/π electron interaction between the phenyl group of the substrates and the phenyl group of the coatings [16–19]. On the other hand, no adhesion was observed for MeTES–TEOS coatings on all the substrates, PET, PC, PE, PP and PVC, and PhTES–TEOS coatings on PE, PP and PVC. This may be attributed to CH_3/π electron interaction and CH_3/CH_3 van der Waals interaction are much smaller than π/π electron interaction [16–21], Further, α in Fig. 7 is always smaller than β in Fig. 9 at the same x, which supports this as well.

Table 3 shows the results of adhesion test of BTEB–TEOS coatings. In comparison with Table 2, note that the adhesion of BTEB–TEOS coatings on PET is 100%, while the adhesion of PhTES–TEOS coatings on PC is 40% at the same $x=60$. The proportion of phenyl group in PET is smaller than that in PC as indicated in Fig. 4; nevertheless the adhesion of BTEB–TEOS coatings on PET is better than that of PhTES–TEOS coatings on PC. This might be attributed to the planar structure of phenyl group held between two Si atoms of BTEB (see Fig. 2) for its good formation of π/π electron interaction.

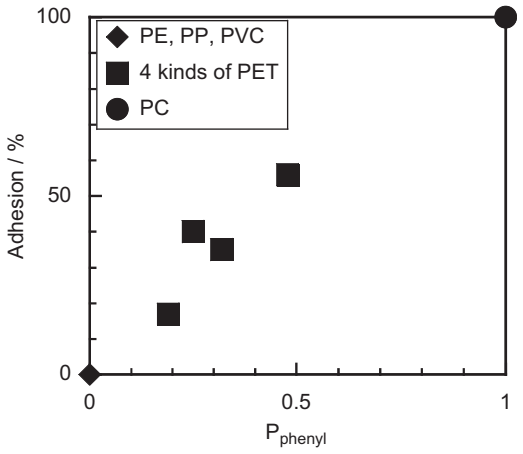

Fig. 11. Relation between the proportion of phenyl group of 8 kinds of plastics substrates and its adhesion.

Table 2
Adhesion of RTES (R=Ph, Me)−TEOS coatings on various plastics substrates.

RTES/ mol%	Adhesion (A)/%									
x RTES−(100−x)TEOS	R=Ph					R=Me				
	PET	PC	PE	PP	PVC	PET	PC	PE	PP	PVC
0	0	0	0	0	0	0	0	0	0	0
20	0	0	0	0	0	0	0	0	0	0
40	0	0	0	0	0	0	0	0	0	0
60	40	100	0	0	0	0	0	0	0	0
80	100	92	0	0	0	0	0	0	0	0

Table 3
Adhesion of BTEB–TEOS coatings on various plastics substrates.

BTEB/mol%	Adhesion (A)/%				
	PET	PC	PE	PP	PVC
0	0	0	0	0	0
20	0	0	0	0	0
40	0	0	0	0	0
60	100	100	0	0	0
80	100	100	0	0	0

4. Conclusion

Organic–inorganic hybrid, xRTES (R=Ph, Me)−(100−x)-TEOS (x=0–80, mol%) coatings were prepared on polyethylene terephthalate (PET), polycarbonate (PC) with phenyl group and polyethylene (PE), polypropylene (PP) and polyvinylchloride (PVC) without phenyl group substrates by sol–gel process and its distribution of organic component and adhesion on the plastics substrates were studied. Distribution of organic component in the coatings was measured using fourier transform infrared (FT-IR) measurement. Concentration of phenyl group on PhTES-TEOS coatings/PET and PC substrates side was larger than that of PE, PP and PVC substrates side at the same x, while concentration of methyl group on MeTES–TEOS coatings/PET and PC substrates side was smaller than that of PE, PP and PVC substrates side at the same x. In other words, the phase separation behavior in the coatings was affected by the plastics substrates. Adhesion on the plastics substrates was observed only for PhTES–TEOS coatings on PET and PC at larger than x=60. This may be attributed to π/π electron interaction between phenyl group in coatings and substrates, which is much larger than that of CH_3/π electron interaction and CH_3/CH_3 van der Waals interaction.

Acknowledgment

We would like to acknowledge the support from Takiron Co., Ltd for supplying PC substrate. This work was supported by Japan Science and Technology Agency (JST) of Adaptable and Seamless Technology transfer Program (A-STEP, AS231Z04429C) and Grants-in-aid for Scientific Research (no. 22550182).

References

[1] D. Katsamberis, K. Browall, C. Iacovangelo, M. Neumann, H. Morgner, Highly durable coatings for automotive polycarbonate glazing, Progress in Organic Coatings 34 (1998) 130–134.
[2] Y.-H. Han, A. Taylor, K.M. Knowles, Scratch resistance and adherence of novel organic–inorganic hybrid coatings on metallic and non-metallic substrates, Surface and Coatings Technology 203 (2009) 2871–2877.
[3] S.K. Medda, D. Kundu, G. De, Inorganic–organic hybrid coatings on polycarbonate: spectroscopic studies on the simultaneous polymerizations of methacrylate and silica networks, Journal of Non-Crystalline Solids 318 (2003) 149–156.
[4] M.E.L. Wouters, D.P. Wolfs, M.C. van der Linde, J.H.P. Hovens, A.H.A. Tinnemans, UV Transparent, curable antistatic hybrid coatings on polycarbonate prepared by the sol–gel method, Progress in Organic Coatings 51 (2004) 312–319.
[5] L.Y.L. Wu, L. Boon, Z. Chen, X.T. Zeng, Adhesion enhancement of sol–gel coating on polycarbonate by heated impregnation treatment, Thin Solid Films 517 (2009) 4850–4856.
[6] Y.J. Shin, D.H. Yang, M.H. Oh, Y.S. Yoon, J.S. Shin, Hard coatings on polycarbonate plate by sol–gel reactions of melamine derivative, poly(vinyl alcohol), and silicates, Journal of Industrial and Engineering Chemistry 15 (2009) 238–242.
[7] N. Nakayama, T. Hayashi, Synthesis of novel UV-curable difunctional thiourethane methacrylate and studies on organic–inorganic nanocomposite hard coatings for high refractive index plastic lenses, Progress in Organic Coatings 62 (2008) 274–284.
[8] M. Dinelli, E. Fabbri, F. Bondioli, TiO_2–SiO_2 hard coating on polycarbonate substrate by microwave assisted sol–gel technique, Journal of Sol-Gel Science and Technology 58 (2011) 463–469.
[9] Y. Mizuta, Y. Daiko, A. Mineshige, M. Kobune, T. Yazawa, Phase-separation and distribution of phenyl groups for PhTES–TEOS coatings prepared on polycarbonate substrate, Journal of Sol-Gel Science and Technology 58 (2011) 80–84.
[10] Y. Mizuta, Y. Daiko, A. Mineshige, T. Yazawa, Solvent effect on distribution of phenyl groups for $C_6H_5SiO_{3/2}$–SiO_2 coatings prepared on polycarbonate substrate, Journal of Sol-Gel Science and Technology 62 (2012) 92–97.
[11] A. Bertoluzza, C. Fanano, M.A. Morelli, V. Gottardi, M. Guglielmi, Raman and infrared spectra on silica gel evolving toward glass, Journal of Non-Crystalline Solids 48 (1982) 117–128.
[12] J. Wong, C.A. Angell, Glass Structure by Spectroscopy, Marcel Dekker, New York, 1976.
[13] Y.-S. Li, Y. Wang, S. Ceesay, Vibrational spectra of phenyltriethoxysilane, phenyltrimethoxysilane and their sol–gels, Spectrochimica Acta Part A. 71 (2009) 1819–1824.
[14] B. Askew, P. Ballester, C. Buhr, K.S. Jeong, S. Jones, K Parris, K. Williams, J. Rebek Jr., Molecular recognition with convergent functional groups. 6. Synthetic and structural studies with a model receptor for nucleic acid components, Journal of the American Chemical Society 111 (1989) 1082–1090.
[15] K. Williams, B Askew, P. Ballester, C. Buhr, K.S. Jeong, S. Jones, J Rebek Jr., Molecular recognition with convergent functional groups. 7. Energetics of adenine binding with model receptors, Journal of the American Chemical Society 111 (1989) 1090–1094.
[16] J. Ran, M.W. Wong, Saturated hydrocarbon-benzene complexes: theoretical study of cooperative CH/π interactions, Journal of Physical Chemistry A 110 (2006) 9702–9709.
[17] S. Tsuzuki, K. Honda, T. Uchimaru, M. Mikami, High-level *ab initio* computations of structures and interaction energies of naphthalene dimers: Origin of attraction and its directionality, Journal of Chemical Physics 120 (2004) 647–659.
[18] S. Tsuzuki, T. Uchimaru, K. Matsumura, M. Mikami, K. Tanabe, Effects of the higher electron correlation correction on the calculated intermolecular interaction energies of benzene and naphthalene dimers: comparison between MP2 and CCSD(T) calculations, Chemical Physics Letters 319 (2000) 547–554.
[19] S. Tsuzuki, K. Honda, T. Uchimaru, M. Mikami, K. Tanabe, Origin of attraction and directionality of the π/π interaction: model chemistry calculations of benzene dimer interaction, Journal of the American Chemical Society 124 (2002) 104–112.
[20] R.C. Thomas, J.E. Houston, R.M. Crooks, T. Kim, T.A. Michalske, Probing adhesion forces at the molecular scale, Journal of the American Chemical Society 117 (1995) 3830–3834.
[21] P.W. Atkins (Ed.), Oxford University Press, Oxford, 1994.